

## Simulation analysis of different bone scaffold porous structures for fused deposition modelling fabrication process

M S Tang<sup>1,\*</sup>, A Z Abdul Kadir<sup>1</sup> and N H A Ngadiman<sup>1</sup>

<sup>1</sup> School of Mechanical Engineering, Faculty of Engineering, Universiti Teknologi Malaysia, 81310 UTM Skudai, Johor Bahru, Malaysia

\*Corresponding email: meishick2207@gmail.com

**Abstract.** Porous structure of bone scaffold plays an important role in tissue engineering applications. The nature of scaffold structure such as porosity, porous structure, pore size and pore interconnectivity can strongly affect the mechanical strength and transportation of nutrients throughout the scaffold in human body. Due to the complexity of internal scaffold structure, Additive Manufacturing (AM) system of Fused Deposition Modelling (FDM) is a promising technology to fabricate scaffold with desired design and properties. In this study, mechanical properties of different Polylactic acid (PLA) porous scaffold porous scaffold designs such as circle and square with pore sizes range 1 mm to 2 mm at targeted porosity of up to 80% were explored. Combination of different shape designs and pore sizes were simulated using ABAQUS. The compressive modulus outcomes of the PLA porous structure for circle and square were in the range of 1.0 to 1.2GPa respectively. Circle porous structure showed better performance, while square porous structure contains sharp edges which produce high concentration stress and resulting to lower elastic modulus. The stiffness increases in combination of different pore sizes which leads to higher Young's Modulus. It should be noted that, the benefits of this simulation analysis may perform preliminary prediction of bone scaffold Young's Modulus before further experimental processes and biological cell proliferation activities. As a conclusion, determination of an ideal scaffold through design and simulation analysis may assist the fabrication of bone scaffold through FDM at enhanced material properties.

**Keywords.** Scaffold; Polylactic-acid; Additive Manufacturing; Fused Deposition Modelling; Scaffold Design; Pore Structure; Tissue Engineering.

### 1. Introduction

Additive Manufacturing (AM) technologies are techniques to create complex structure by addition of material layer by layer. AM is an office-friendly technique where 3D parts were created using CAD model, then converts to a .stl format file of the part to be printed as input data [1]. AM has been widely used in Tissue Engineering (TE) application due to design freedom, various material choices, multiple material, minimum material wastage and decreased lead times. For example, complex internal porous structure in TE scaffold can be manufactured using different AM processes, by only modifying the CAD design based on innovativeness of designers [2]. However, the design of internal porous structure and material used could strongly affect the mechanical properties of scaffold and the transportation of

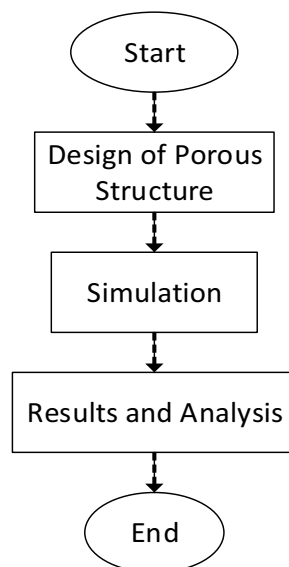


nutrients and metabolic waste products throughout the scaffold in the body [3]. Therefore, pore size should be at least 100 microns to allow the movement of nutrients and porosity range of above 75% to improve bone growth, nutrient transportation, and degradation rate of the scaffold in human body [4, 5]. However, large pore size and porosity range decrease the mechanical performance. Therefore, researcher repeatedly investigate the suitable pore sizes with high percentage of porosity range due to the demands of tissue engineering regeneration. Scaffold structure contains porosity, pore structure, pore size and pore interconnectivity which can strongly affect the transportation of nutrients and metabolic waste products throughout the scaffold in the body [3]. Pore structure can be obtained in a cubical scaffold in three directions (x, y, and z axis) with repeating interconnected unit cell or periodic arrangement of the voids which also called as periodic cellular structure. Periodic cellular structure has better energy absorption and acoustic insulation properties compared with random distribution interconnected unit cell and allows nutrients and fluid transportation in the fabricated scaffold [2].

In this paper, ideal porous design and desired porosity scaffold were investigated, which focused on Young's Modulus mechanical properties analysis of the developed scaffold design. Young's Modulus was analyzed for the selection of material and structure in replacement of human bones implants. A polylactic acid (PLA) biomaterial filament was used as the material in Fused Deposition Modelling (FDM) AM process. The mechanical properties were simulated using Finite Element Analysis (FEA) in ABAQUS software. Two designs of porous structure, circle and square with various porous scaffold sizes were modelled using SOLIDWORK. The combination of macro and micro porous sizes was also studied. Three axis of periodic cellular structure scaffold with pore size of 1000 microns at over 80% porosity was designed in order to develop an AM-based scaffold with ideal mechanical properties.

## 2. Methodology

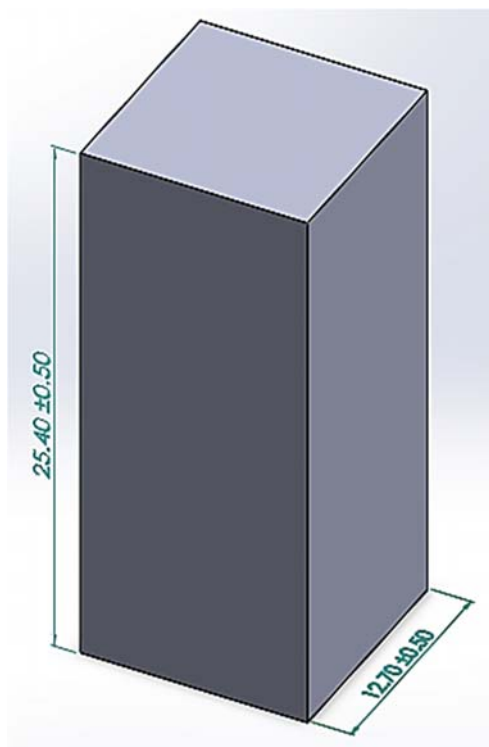
General flow chart of the methodology is shown in figure 1. The section starts with sample preparation followed by CAD design methods of the porous structure and finally simulation analysis techniques. The porous structure scaffold was first designed using SOLIDWORKS with circle and square pore shapes. Then the drawings undergone simulation using ABAQUS 6.14-1 to obtain the Young's Modulus. The results were then documented and compared with the outcomes of literature in order to obtain ideal scaffold designs. Detail descriptions of these methods are discussed in the following sub-sections.



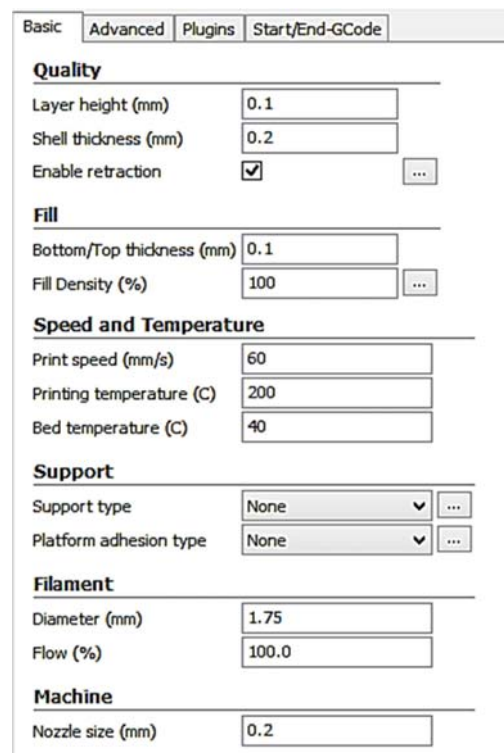
**Figure 1.** Flowchart methodology.

### 2.1. Sample preparation

The scaffold was first designed based on ISO 604 standard for compression testing. The specimen dimension is a rectangular cube shaped polymer of 12.7 mm x 12.7 mm x 25.4 mm (Figure 2). Polylactic acid (PLA) is one of the materials for FDM which was found to be biodegradable and biocompatible for living cells. Five samples of full solid PLA were fabricated by FDM process. FDM machine of Creality Ender 3 an open source machine, was used to fabricate the solid PLA. Next, slicing application software, CURA, was used to import the .STL files and the setting of machine parameters. Samples were printed with 100% infill percentage, temperature of 200 °C and 60 mm/s printing speed. Figure 3 shows the machine parameter setting of the CURA software. Tests were performed to obtain the Young's Modulus, Poisson ratio and density. The data collection from this experiment were then inserted in the material properties of ABAQUS simulation analysis in the following stage



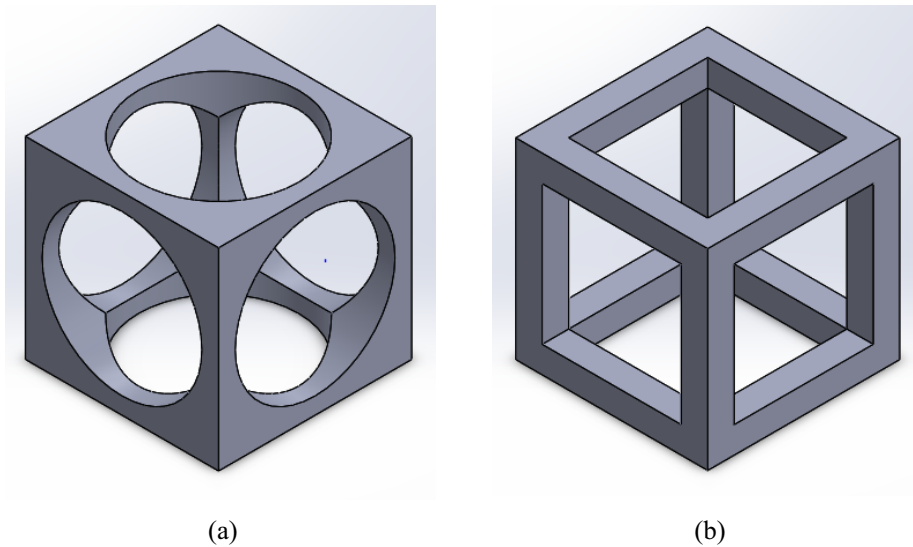
**Figure 2.** Solid cube design and its dimension.



**Figure 3.** Machine parameters setting to fabricate solid PLA samples.

### 2.2. CAD design of porous structure

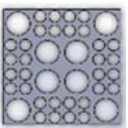
The porous structure of the bone scaffolds was designed using SOLIDWORKS having a unit cell with enclosed dimension of 12.7 mm x 12.7 mm x 12.7 mm for both circle and square shapes. Several trial and errors were performed to obtain the porosity to be constant at 81% for both designs. Initial designs of circle and square porous structure were investigated with the increasing number of porous cells from 1, 2, 4 and 8 in each direction in order to create smallest porous size for FDM fabrication. The dimension was in accordance to ISO standard (ISO 604) of length and width, where the height is twice of a unit which is equals to 25.4 mm. Figure 4 shows the CAD model of the circle and square porous structure in a unit cell.



**Figure 4.** Porous structure in a unit cell of (a) Circle; and (b) Square shapes.

There were five sample designs used in the simulation analysis and the characteristics such as their cell dimensions, porous volume, volume enclosed, surface area and SA/V ratio, are shown in table 1. The combination of macro and micro size, and the combination of circle and square porous structures were compared. All the designs porosity recorded a porosity at over 80%. The pore size was maintained at 1215 micron to 1313 micron for micro pore size, and 2250 to 2625 micron for macro pore size.

**Table 1.** Characteristic sample design.

Model Name	S4	C4	CS	SS	CC
Designs					
	Square porous	Circle porous	Circle and square porous	Macro and micro of square porous	Macro and micro of circle porous
Dimension of a cell size, mm	L= 1.5875 l = 1.125	L= 1.5875 d = 1.3125	Circle L= 1.5875 d = 1.3125 Square L= 1.5875 l = 1.125	Macro L = 3.175 d = 2.625 Micro L= 1.5875 d = 1.3125	Macro L = 3.175 l = 2.25 Micro L= 1.5875 l = 1.125
Porous volume, mm <sup>3</sup>	3334.82	3323.94	3338.23	3377.08	3412.04
Volume enclosed, mm <sup>3</sup>	4096.77	4096.77	4096.77	4096.77	4096.77
Surface area, mm <sup>2</sup>	6948.90	5887.76	6457.74	5090.40	4520.45
SA/V ratio	2.08	1.77	1.93	1.51	1.32

2.3. *Simulation analysis*

The porous structure scaffolds were simulated using ABAQUS 6.14-1 software in order to find the Young’s Modulus of various scaffold designs. At first, the models from SOLIDWORKS software were imported. Next, the material properties were manually added inside the property side of the module. Young’s Modulus, Poisson ratio and density from the experimental solid PLA were used in order to get accurate simulation results. For the boundary condition, lower part of the scaffold design was fixed, and the upper part was compressed at about 5% of its height. The time of period was set at 1s with an increment of 0.01s.

The mesh independence test was conducted by using a unit cell of square and circle porous structures analysis from 1.7 mm to 0.3 mm global seed. Global seed is a size of element used during meshing. The simulation was then repeated several times with different sizes of global seed in order to achieve mesh independence. The percentage difference must be less than 5% compared to the previous global seed of Young’s Modulus values [7]. When the simulation is completed, the structure was rendered in different colours to show the safety level of the samples (Figure 5). The stress-strain values were recorded to find the Young’s Modulus and graph plotting.

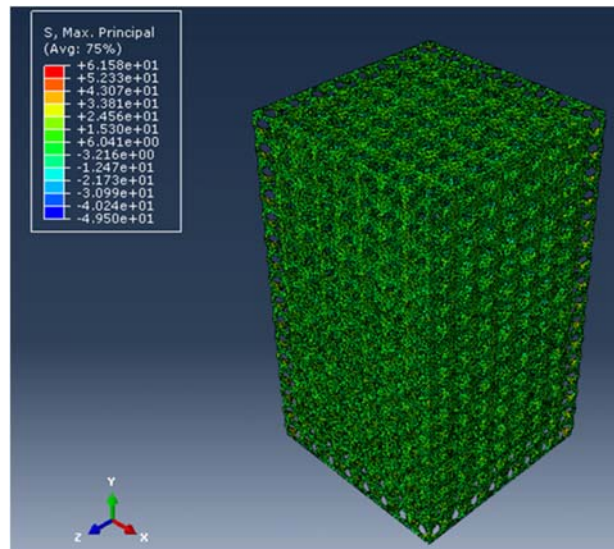


**Figure 5.** Colour gradient in C4 sample during simulation

3. **RESULTS AND DISCUSSION**

The results of mesh independence and mechanical performance are presented in this section. Besides, the percentage of porosity for five different designs were also discussed. Data collection from the simulation are focused on Young’s Modulus of the scaffold structure.

3.1. *Percentage of Scaffold porosity*

The trial and errors of obtaining the correct dimensions of porous structure either in circle or square designs, led to porosity range of above 81% (Table 2) for all the five designs. Combination of macro and micro porous structure showed higher porosity compared with the other three designs. This is probably due to the extrude cut of different pore sizes which makes the porous volume increased.

**Table 2.** Porosity percentage of five designs.

Designs	S4	C4	CS	SS	CC
Porosity (%)	81	81	81	82	83

3.2. Mesh independence test

Table 3 and table 4 show the mesh independence test results of circle and square porous structure ranging from 1.7 mm to 0.3 mm global seed. As mentioned in the previous sections, mesh independence test was performed, and 0.3 mm global seed was obtained for all simulated scaffold designs. At around 0.3 mm global seed the value of Young’s Modulus for circle and square porous were 423.99 MPa and 715.78 MPa, respectively, which fulfilled the mesh independence in both structures. It was also found that the Young’s Modulus dropped to 81% and 68%, respectively from solid PLA Young’s Modulus value of 2238.42 MPa.

**Table 3.** Mesh independence test for circle porous.

Global Seed (mm)	Number of elements	Young Modulus (MPa)	Percentage (%)
1.70	1554	659.13	-
1.30	3506	694.60	5.11
0.80	13302	711.87	2.43
0.35	126706	715.78	0.55

**Table 4** Mesh independence test for square porous.

Global Seed (mm)	Number of elements	Young Modulus (MPa)	Percentage (%)
1.70	1280	470.37	-
1.00	5961	432.35	8.08
0.50	46144	427.81	1.05
0.30	213177	423.99	0.89

From the result, both Young’s Modulus values dropped to 81% and 68% respectively from solid PLA Young’s Modulus value. Overall, the differences between each global seed result showed decreasing in percentage. The smaller the global seed will increase the number of elements. In order to achieve mesh independence, the percentage differences could not be more than 5%. However, large elements provide longer computing time, but the data computed will be more precise. Therefore, mesh independence test advantage in determine the correct number of elements that need to be used in simulation.

Figure 6 shows the mesh independence test results for circle and square porous structures. Line graph showed the circle and square porous structure has achieved the mesh independence. The differences of the percentage between each global seed were decreased to 0.89%. As mentioned, smaller global seed showed more accurate data. Therefore, 0.3 mm global seed were chosen to use in all model designs.

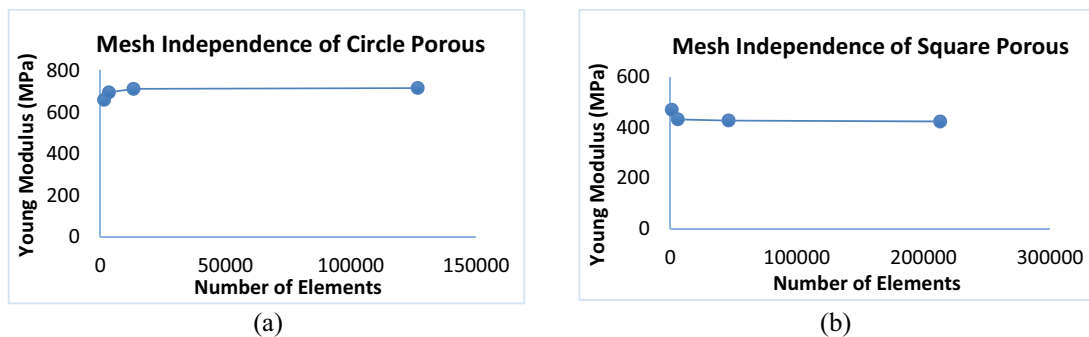


**Figure 6.** Mesh independence test for (a) Circle; (b) Square porous structure.

### 3.3. Simulated Young's Modulus results

Simulated results of Young's Modulus for the five sample designs are shown in table 5. Value of the solid PLA was also stated in the table for comparison. From the table, S4 and C4 dropped to 1030 MPa (54%) and 1147.89 MPa (49%), respectively from the Young's Modulus of solid PLA. Combination of circle and square porous structures were slightly lower than S4 and C4 which is 1015.42 MPa. Combination of different pore size of circle and square porous structure showed higher results. Detailed discussions are discussed in the following subsections.

**Table 5.** Young's Modulus of five different designs

No.	Model Name	Young's Modulus (MPa) (Avg)
1.	Solid PLA	2238.42
2.	S4	1030.00
3.	C4	1147.89
4.	CS	1015.42
5.	SS	1145.17
6.	CC	1272.42

### 3.4. Comparison of different pore structures using Abaqus

In this study, the shapes of porous structure were investigated with over 80% porosity. In the simulation, 5% of the scaffold height was compressed in order to find the Young's Modulus. From figure 7, it shows that the stress-strain curve of circle porous structure was steeper than the square porous structure. This indicated that more stress was needed to stretch the circle porous compared to the square porous structure. Furthermore, square porous contains edgy geometry, where the sharp edge will produce high concentration stress which performed in low elastic modulus [8]. Therefore, results showed the circle porous structure obtained better elastic modulus compared with to square porous structure.

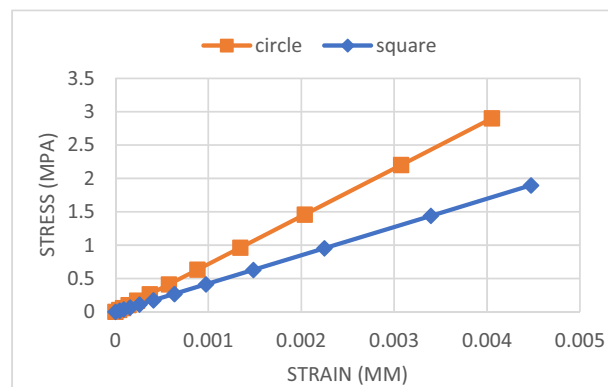


**Figure 7.** Stress-strain curve for circle and square porous structures.

Figure 8 shows a bar chart of the difference on Young's Modulus between sample S4, C4 and CS. As mentioned in the previous section, comparison with combination structure CS porous sample, the Young's Modulus showed slightly decreased. This is due to the neck region between the square and circle porous was thinner than other porous designs. Moreover, the diameter and length of both designs were different, where circle porous structure was larger than the square porous structure to make it in the same range of porosity. This caused the lower radius of strut to produce lower Young's Modulus [9]. Besides, sharp edges shown in figure 9 of the square will also influence the strength of the structure.

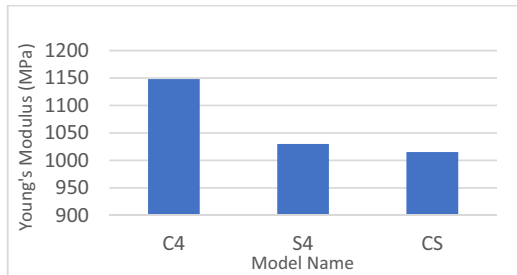


**Figure 8.** Young's Modulus of sample C4, S4 and CS.

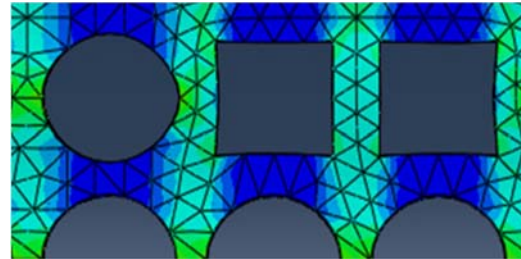


**Figure 9.** The combination of circle and square porous structures.

*3.5. Comparison of macro and micro pores structure*

Recent study showed that the combination of macro, micro and even nano-sized pore sizes have better results in mechanical strength and cell generation compared to single macro pore size [10, 11]. It was also proved that combination of macro and micro pore sizes have better mechanical properties than micro pore size in circle and square porous structure. Besides, this design increases the complexity level of scaffold framework which allows bone regeneration in the advantage of specific boundary and loading conditions of the bone construct. Figure 10 shows a bar chart of Young's Modulus results for, (a) circle porous (C4) and the combination of macro and micro circle pore structure (SS); and (b) square porous (S4) and the combination of macro and micro square pore structure.

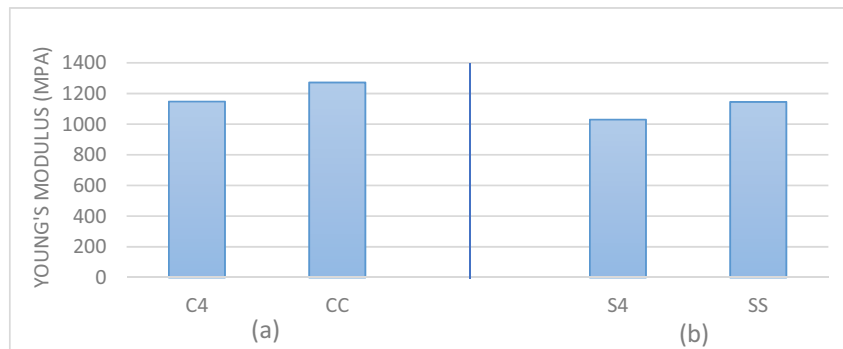


**Figure 10.** Young's Modulus of (a) C4 and CC; (b) S4 and SS.

From figure 10, it can clearly be seen that both designs have higher Young's Modulus after the combination of different pore sizes. As mentioned in Section 3.3, sample CC increases to 124.53 MPa compared with C4, while SS increases 115.17 MPa compared with S4. This is due to different sizes of pore structures are cut away in the dense PLA cube, where the remain solid area becomes dominate in the transmission of stress throughout the whole body [12]. However, micro size pore structure influences the crack propagation dramatically, but this showed less effect on the fracture of pore walls. The failure of cracking of the neck area of the scaffold is controlled by macro sized pores [13]. Figure 11 shows the arrangement of macro and micro size of circle pore structure. Therefore, larger struts area produced by the macro size structure increases the stiffness which leads to high Young's Modulus.

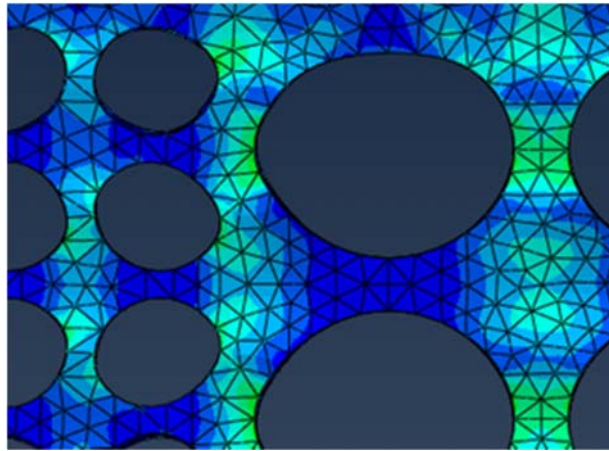


**Figure 11.** Stress diagram of macro and micro size circle pore structure (CC).

Besides, Young's Modulus results from this study were within the range of physical and mechanical properties of cortical and cancellous bone for PLA scaffold. Young's Modulus of cortical bone recorded a range of 1 to 20 GPa and strength in a range of 1-100 MPa, while cancellous bone on the other hand recorded a range of 0.1 to 1.0 GPa and strength between 1 to 100 MPa [12, 13]. In a similar study by Jalil and Todo (2017), the investigation of square and hexagonal pore sizes with porosity of 80% in only y-axis direction resulted that 1.0 mm diameter pore structure dropped to 39% compared to solid PLA Young's Modulus value [16]. On the other hand, hexagonal and gyroid shape of PDLLA scaffold with the porosity of 55% to 70% were also recorded by Olivares *et al.* (2009). The highest simulation results of Young's Modulus for hexagonal 55% were achieved to 1514 MPa [17]. Table 6 shows the comparison between current study and the summarized outcomes of previous research. Therefore, the simulation results from this study achieved in the range of scaffold desired properties. High porosity and Young's Modulus of PLA scaffold were created which were comparable to cortical bone. Combination of different pore sizes and pore designs scaffold showed an enhancement in the mechanical properties.

**Table 6.** Comparison of various mechanical properties with previous studies.

No.	Ref.	Porous Designs	Axis	Porosity	Young's Modulus
1.	Jalil and Todo, (2017) [16]	Square and Hex	y-axis	80%	Young's Modulus of square 1.0 mm and Hexagonal 1.0 mm are 1000 MPa and 790 MPa.
2.	Olivares <i>et al.</i> , (2009) [17]	Hex and Gyroid	x and y-axis	55% - 70%	Young's Modulus of Hexagonal 55% reached highest value of 1514 MPa.
3.	Current Study	Square and Circle	x, y and z-axis	80%	Young's Modulus are recorded at 1.0 to 1.2GPa.

#### 4. Conclusion and future work

The mechanical properties such as Young's Modulus for two designs of pore structure with circle and square shapes were simulated using ABAQUS 6.14-1 in preparation for bone scaffold fabrication. In order to performed better scaffold fabrication with porous structures at more than 80% porosity level,

fused deposition modeling (FDM) technique was first used to fabricate the solid cube designs. From the simulation, circle porous structure showed higher properties values than the square porous structure. When comparing with the combination of different pore size structure (SS and CC), the Young's Modulus increased. It can be concluded that, large dimension of neck region between macro and micro pore size increase the value of Young's Modulus. However, combination of different design pores (circle and square) resulting slightly lower Young's Modulus. Furthermore, all the different types of pore designs recorded only small differences with each other. It was proved that the simulation analysis can assist in performing preliminary prediction before the actual fabrication of porous scaffold structure takes place. The study concluded that, Young's Modulus property can be varied by changing the different pore designs using various shapes and the combination of desired pore sizes. These results could also enhance researcher for further research and development in the field of tissue engineering for scaffold fabrication.

Future work will utilize the simulation results for further development of bone scaffold at various designs, shapes, and porosity level as well biological cell proliferation with the aim of ideal bone scaffold development.

#### Acknowledgement

The authors wish to acknowledge the funding supports from Research University Grant (RUG), Universiti Teknologi Malaysia (UTM) (Vot. No. 06G11 and 20H47) as well as UTM National Postgraduate Fund, (NPF), Malaysia.

#### References

- [1] Gardan J Makke A and Recho N 2016 *A Method to Improve the Fracture Toughness Using 3D Printing by Extrusion Deposition* vol 2 (Struct. Integr. Procedia) pp 144-151
- [2] Parthasarathy J Starly B and Raman S 2011 *A design for the additive manufacture of functionally graded porous structures with tailored mechanical properties for biomedical applications* vol 13 (J. Manuf. Process.) pp 160-170
- [3] Schüller-Ravoo S Teixeira S M Feijen J Grijpma D W and Poot A A 2013 *Flexible and elastic scaffolds for cartilage tissue engineering prepared by stereolithography using poly(trimethylene carbonate)-based resins* vol 13 (Macromol. Biosci.) pp 1711-1719
- [4] Bose S Vahabzadeh S and Bandyopadhyay A 2013 *Bone tissue engineering using 3D printing* vol 16 (Biochem. Pharmacol.) pp 496-504
- [5] Loh Q L and Choong C 2013 *Three-Dimensional Scaffolds for Tissue Engineering Applications: Role of Porosity and Pore Size* vol 19 (Tissue Eng. Part B Rev.) pp 485-502
- [6] Torres J Cotel J Karl J and Gordon A P 2015 *Mechanical property optimization of FDM PLA in shear with multiple objectives* vol 67 (JOM) pp 1183-1193
- [7] Moinuddin K A M and Thomas I R 2007 *Factors Affecting Grid-independent Results for Compartment Fire Modelling* (16th Australasian Fluid Mechanics Conf.) pp 1254-1257
- [8] Budynas R G and Nisbett J K 2014 *Shigley's Mechanical Engineering Design (McGraw-Hill Series in Mechanical Engineering)*. ed McGraw-Hill Education
- [9] Bagheri A Buj-corral I Ballester M F and Pastor M M 2018 *Determination of the Elasticity Modulus of 3D-Printed Octet-Truss Structures for Use in Porous Prosthesis Implants* vol 11 (Materials) p 2420
- [10] Boccaccio A Uva A E Fiorentino M Mori G Monno G 2016 *Geometry Design Optimization of Functionally Graded Scaffolds for Bone Tissue Engineering: A Mechanobiological Approach* *PLoS ONE* **11** 0146935
- [11] Woodard J R Hilldore A J Lan S K Park C J Morgan A W Eurell J A C Clark S G Wheeler M B Jamison R D 2007 *The mechanical properties and osteoconductivity of hydroxyapatite bone scaffolds with multi-scale porosity* vol 28 (Biomaterials) pp 45-54
- [12] Esen Z and Bor S 2007 *Processing of titanium foams using magnesium spacer particle* vol 56 (Scripta Materialia) pp 341-344

- [13] Li B Q Wang C Y and Lu X 2013 *Effect of pore structure on the compressive property of porous Ti produced by powder metallurgy technique* vol 50 (Materials and Design) pp 613–619
- [14] Gregor A Filova E Martin N Jakub K Hynek C Buzgo M Veronika B Lukasova V Martin B Alois N Hosek J 2017 *Designing of PLA scaffolds for bone tissue replacement fabricated by ordinary commercial 3D printer* vol 11 (J. Biol. Eng.) pp 1–21
- [15] Lee S Porter M Wasko S Lau G Chen P Novitskaya E E Tomsia A P Almutairi A Meyers M A Mckittrick J 2012 Potential Bone Replacement Materials Prepared by Two Methods *MRS Proc.* **1418** (Mrsf11-1418-mm06-02)
- [16] Jalil M H and Todo M 2017 *Development and Characterization of Gear Shape Porous Scaffolds Using 3D Printing Technology* vol 7 (Int. J. Biosci. Biochem. Bioinforma.) pp 74–83
- [17] Olivares A L Marsal E Planell J A and Lacroix D 2009 *Finite element study of scaffold architecture design and culture conditions for tissue engineering* vol 30 (Biomaterials) pp 6142–6149